EUROPEAN ORGANIZATION FOR NUCLEAR RESEARCH

CERN–PPE/95–157
26 October 1995

Low p_T Phenomena in A+A and p+A Collisions at Mid-rapidity

H. Bøggild[1], J. Boissevain[2], M. Cherney[3], J. Dodd[4], S. Esumi[5], C.W. Fabjan[6], D. E. Fields[2], A. Franz[6], E.B. Holzer[6], T. Humanic[7,a], B.V. Jacak[2], R. Jayanti[7,a], H. Kalechofsky[7,b], R. Kvatadze[6,c], Y.Y. Lee[7,d], M. Leltchouk[4], B. Lorstad[8], N. Maeda[5], A. Medvedev[4], A. Miyabayashi[8], M. Murray[9], S. Nishimura[5], E. Noteboom[3], S.U. Pandey[7,a], F. Piuz[6], V. Polychronakos[10], M. Potekhin[4], G. Poulard[6], A. Sakaguchi[5], M. Sarabura[2], J. Schmidt-Sorenson[1], J. Simon-Gillo[2], W. Sondheim[2], M. Spegel[6], T. Sugitate[5], J. P. Sullivan[2], Y. Sumi[5], H. van Hecke[2], W.J. Willis[4], K.Wolf[9], N. Xu[2]

[1] Niels Bohr Institute, DK-2100 Copenhagen, Denmark.
[2] Los Alamos National Laboratory, Los Alamos, NM 87545, USA.
[3] Creighton University, Omaha, NE, USA
[4] Columbia University, New York, NY 10027, USA.
[5] Hiroshima University, Higashi-Hiroshima 724, Japan.
[6] CERN, CH-1211 Geneva 23, Switzerland.
[7] University of Pittsburgh, Pittsburgh, PA 15260, USA.
[8] University of Lund, S-22362 Lund, Sweden.
[9] Texas A&M University, College Station, TX 77843, USA.
[10] Brookhaven National Laboratory, Upton, NY 11973, USA.
[a] Now at Dept. of Physics, Ohio State University, Columbus, OH 43210, USA
[b] Now at University of Geneva, Geneva, CH-1211, Switzerland.
[c] Visitor from Tbilisi State University, Tbilisi, Rep. of Georgia.
[d] Now at GSI Laboratory, Darmstadt, D-6100, Germany.

NA44 Collaboration

Abstract

CERN experiment NA44 measures pion and kaon distributions at p_T = 0-320 MeV/c at midrapidity in p+A and A+A collisions at 450 and 200A GeV/c, respectively. Pion production from p+Pb and A+A is slightly enhanced at low p_T relative to p+Be, but less than observed at target rapidity. The low p_T behavior can be understood in the context of the RQMD model as arising from baryonic resonance decays.

(Accepted by Z. Phys. C)

1 INTRODUCTION

Experiments have reported an enhancement in pion production at low p_T ($<$ 300 MeV/c) compared to minimum bias pp results. This excess was observed at the ISR in high multiplicity pp and $\alpha\alpha$ collisions [1], in cosmic ray data [2], in p+A (Fermilab, CERN) [3, 4, 5, 6] and in A+A collisions (AGS, CERN) [5, 6, 7, 8, 9, 10]. Intriguing explanations, including exotic behavior in dense hadronic matter [11, 12, 13], the decay of quark matter droplets [14], collective effects [2, 15], and baryonic and mesonic resonance decay [7, 16, 17, 18], have been proposed. We have studied the rapidity dependence of the low p_T enhancement in attempt to understand the source of the behavior.

CERN experiment NA44 is a focussing spectrometer, optimized for the study of identified single and multiple particle distributions at mid-rapidity. The spectrometer has particle identification at the trigger level and achieves a high data rate. We measure p+Be (as an approximation to p-p) and p-nucleus collisions at 450 GeV/c, and nucleus-nucleus collisions at 200A GeV/c in the same experiment to characterize the low p_T enhancement and distinguish among the proposed explanations.

Comparing positive and negative pion spectra allows a search for evidence of Coulomb repulsion/attraction from the emitting source which would be most evident at low p_T. This effect would manifest itself as a low p_T enhancement in the π^- p_T distribution as compared to the π^+ p_T distribution and has been reported in the baryon-rich environment at the AGS [10].

A search for enhanced production of low p_T kaons, which are less affected by resonance decay, can help differentiate among the possible explanations of the low p_T pion excess. In addition, excess low p_T kaon production could signal chiral symmetry restoration in the collisions [19, 20].

2 EXPERIMENT

The focussing spectrometer uses three quadrupole and three dipole magnets. The momentum range selected by the spectrometer covers a band of $\pm$ 20% around its nominal momentum setting; results from 4 GeV/c pions and 8 GeV/c kaons measured with our low p_T spectrometer angle setting are presented here. The angular coverage is approximately -0.3° to 4.5° in the horizontal and $\pm$ 0.3° in the vertical plane. Only one charge state is detected at a time. The spectrometer uses three highly segmented scintillator hodoscopes which provide tracking information and time-of-flight for each particle.

Two threshold Cherenkov counters allow trigger level particle identification and elimination of conversion electron contamination. The first discriminates π from K and p or π and K from p, and the other identifies electrons. A uranium-scintillator calorimeter, which was not used in this analysis, separates e, π, and μ.

A scintillator just beyond the target is used to trigger on minimum bias (at least one minimum ionizing particle) or central collisions (large particle multiplicity). A silicon pad detector measures the charged-particle multiplicity with 2π azimuthal acceptance and pseudorapidity $1.5 < \eta < 3.3$. A simulation requiring a hit in the trigger counter selects approximately 86% of all p+Be interactions. A sample of peripheral S+Pb collisions is selected from minimum bias data; the peripheral collisions correspond to approximately 58% of the total cross section. Central S+Pb and S+S collisions correspond to the top 9% and 14% of the total cross section, respectively.

The times from all three hodoscopes are used for particle identification; the time resolution is $\approx$80ps with a maximum flight path from the target of 18m. The beam rate and time-of-flight start signal are determined using a Cherenkov beam counter with time resolution of 35ps in A+A collisions [21]. For p+A collisions, a scintillator with time resolution of 100ps is utilized for the time-of-flight start signal in p+A collisions. The experiment has been described in detail elsewhere [22].

Tracks are reconstructed from hit positions on the three hodoscopes, constrained by the target position and straight-line trajectories after the magnets. The particle identification from both time-of-flight and the Cherenkov counters is used. Pions are in the rapidity range y_{lab}=3-4 and kaons in the range y=2.5-3. The p_T distributions are corrected for geometrical acceptance, reconstruction inefficiencies, multiple scattering effects, and decays in flight. The momentum scale is known to 1.6% and the p_T resolution for the 4 and 8 GeV/c momenta settings is 12 and 24 MeV/c, respectively; the systematic error on the p_T scale is approximately 7 MeV/c. Contamination of the pion spectra by electrons or kaons is less than one percent. Contamination of the kaons by electrons and pions is also at the 1% level, and contamination by protons a few percent. Empty target contributions were observed not to affect the shape of the distributions, and consequently, such corrections were not included. As the data are presented as ratios of p_T spectra in different projectile-target combinations, other systematic errors cancel.

3 Results

As shown in figure 1, the measured pions span a unit of rapidity. The results have been corrected for the rapidity dependence of dN/dy in our acceptance using the RQMD model (Relativistic Quantum Molecular Dynamics) [23]. The p_T distributions of hadrons from RQMD have been shown to agree well with various experimental data [24]. The dN/dy corrections were also calculated with the FRITIOF event generator [25]; within errors, these corrections agreed with the RQMD generated corrections. It is well known that resonances strongly influence the p_T distribution of hadrons. The RQMD event generator includes hadronic rescattering as well as the excitation of strings and resonances, and offers a tool to quantify the effect.

We must differentiate between an effect from the shift in center-of-mass between p+A and A+A collisions and the existence of low p_T enhancement. Particle p_T distributions measured from pp collisions at the ISR show little dependence of inverse slopes on $\sqrt{s}$ in the range of 23-31 GeV [26]. The data measured by Guettler et al. show a 4±2% increase in the low p_T region (0-320MeV/c) when the pion distribution at $\sqrt{s}$=31 is compared to the distribution measured at $\sqrt{s}$=29 GeV [27]. RQMD events were used to generate pion and kaon p_T distributions from p+Be and p+Pb collisions at both 200 and 450 GeV/c; within errors, the inverse slopes did not change with beam energy.

The data presented in this paper are in the range $0 \leq p_T \leq 320$ MeV/c. Results are presented as ratios of p_T distributions of heavier systems to those of lighter systems. This is preferable to fitting the p_T distribution, as the fit parameters depend on the fitting procedure chosen and the p_T range. In addition, it is difficult to fit the NA44 data to extract the fraction of soft pions in the low p_T region because the enhancement is small and the spectrum nearly exponential within the acceptance of our experiment.

Two calculations are performed to quantify the the low p_T behavior. In the first method, the magnitude of the low p_T enhancement is determined via:

$$\frac{\int_0^{240MeV/c} p_T dp_T [K(dN/p_T dp_T dy)_A - (dN/p_T dp_T dy)_B]}{\int_0^{\infty} p_T dp_T (dN/p_T dp_T dy)_B} \quad (1)$$

where the subscripts A and B refer to the p_T distributions in the numerator and denominator of the ratio, respectively. The constant K is defined to force agreement in the normalizations of the two p_T distributions $(K(dN/p_T dp_T dy)_A$ and $(dN/p_T dp_T dy)_B)$ in the range $240 \leq p_T \leq 320$ MeV/c. An excess of soft pions has been observed previously below center of mass rapidity at $p_T < 300$ MeV/c, so changes in the ratio would be expected in this region. The integral in the denominator extrapolates to $p_T = \infty$ using an exponential p_T distribution with a slope parameter determined from the data. The contribution from the extrapolation is typically $\approx 40\%$ of the value of the integral in the denominator.

In the second method, the ratio of the p_T distributions is normalized to the average and fit with a horizontal line through unity to test the hypothesis that there is no excess; the resulting χ^2 per degree of freedom values (χ^2/N) are listed in table 1.

GEANT [28] simulations were performed to study low p_T pion production from Λ and K_s^0 decaying into our acceptance. The simulations showed that the contribution of π^- from Λ decay is on the order of 1% and π^+ from $\overline{\Lambda}$ decay on the order of 0.2%. Overall, the pions from K_s^0 decay represent an increase of 7.34 $\pm$0.33% in the total number of reconstructed pions per event in our acceptance. However, in order to create a low p_T enhancement, the pions from K_s^0 decay must have a different p_T spectrum than that of the primary pions in our acceptance. A plot of the ratios of the p_T distributions of primary pions+pions from K_s^0 decays relative to primary pions is shown in figure 2. There is no departure from unity.

Figure 3 shows the ratio of the p_T distributions from central S+Pb $\rightarrow \pi^-$ and central S+Pb $\rightarrow \pi^+$. The shaded area in figure 3 represents the statistical uncertainty in the normalization to $240 < p_T < 320$ MeV/c and dominates the error associated with the calculated difference. The low p_T region in π^+ differs from π^- by 2.8 $\pm$ 1.3%; the χ^2 per degree of freedom of 1.9 indicates no substantial deviation from unity.

Table 1: χ^2 per degree of freedom (χ^2/N where $N = 7$) for the ratios of p_T distributions that have been normalized to the average and fit to a line at unity.

	$\frac{SPb\rightarrow\pi^-}{SPb\rightarrow\pi^+}$	$\frac{SPb\rightarrow\pi^-(cen)}{SPb\rightarrow\pi^-(per)}$	$\frac{SPb\rightarrow\pi^-}{pBe\rightarrow\pi^-}$	$\frac{SS\rightarrow\pi^-}{pBe\rightarrow\pi^-}$	$\frac{pPb\rightarrow\pi^-}{pBe\rightarrow\pi^-}$	$\frac{SPb\rightarrow\pi^-}{pPb\rightarrow\pi^-}$
χ^2	1.9	3.1	3.9	1.4	2.9	1.1

Figure 4 shows the ratio of the p_T distributions of central S+Pb $\rightarrow \pi^-$ and peripheral S+Pb $\rightarrow \pi^-$. The χ^2/N is 3.1 and the magnitude of the enhancement is 6.6 $\pm$ 1.6%, indicating a small difference between central and peripheral collisions.

Figure 5 shows the ratios of π^- production as a function of p_T for different projectile-target combinations. The soft pion excesses, before and after the correction for dN/dy variations within our acceptance, are listed in table 2; the dN/dy corrections essentially double the observed excess. The χ^2/N for each of the ratios is listed in table 1. A small enhancement is visible at low p_T in the A+A/p+Be results; p+Pb shows an enhancement over p+Be, similar in magnitude to S+Pb/p+Be.

The ratios of central S+Pb$\rightarrow K^-$ and minimum bias p+Pb$\rightarrow K^-$ production to minimum bias p+Be$\rightarrow K^-$ are shown in figure 6. The K^- A+A/p+A ratios show a decrease in the low p_T region which is consistent with the difference in the inverse slopes for kaons in p+A and A+A collisions [29]. The K^- slopes in A+A collisions are larger than in p+A and correspond to a decrease in the low p_T region when determining the ratios. This behavior complicates the usage of ratios to quantify a low p_T enhancement in

Table 2: Observed low p_T excess for ratios of various projectile-target combinations, with and without the RQMD dN/dy corrections.

	$\frac{S+Pb}{p+Be}$	$\frac{S+S}{p+Be}$	$\frac{p+Pb}{p+Be}$	$\frac{S+Pb}{p+Pb}$
with correction	11.2±4.4%	9.1±5.3%	8.3±4.0%	2.5±4.2%
without correction	4.9±1.9%	11.4±1.9%	4.2±1.9%	0.7±1.9%

kaon data and decreases its sensitivity to small enhancements. However, if a significant low p_T enhancement exists, the ratio would increase at lower p_T. Furthermore, knowing the inverse slopes of the p_T distributions, one can calculate the sensitivity of the approach to an enhancement with a given slope. For example, an additional component in the kaon spectrum with an inverse slope of 50 MeV/c would be visible in the ratio we construct if the enhancement is 3.5% or greater. The sensitivity improves as the inverse slope parameter decreases. The fact that the ratios smoothly decrease suggests no anomalies at low p_T. In addition, the p+Pb/p+Be ratio in figure 6 is flat, contrary to the similar plot shown for pions in figure 5. The shape of the K^+ p_T distribution is similar to the K^- [30]. It should be noted that, unlike kaons, the pion inverse slopes do not differ significantly from p+A to A+A [29].

4 Discussion

The NA44 results extend the rapidity range at CERN energies to $y = 4$, so we may study the rapidity dependence of soft pion production. The pion low p_T enhancement in NA44 is smaller than that reported by HELIOS and NA35, which both measure nearer to target rapidity. NA35 has demonstrated that the low p_T enhancement increases with decreasing rapidity [31, 7]. Pion data from several CERN experiments were fit with a sum of two exponentials in m_T to estimate the fraction of soft pions, showing that the enhancement is largest at backwards rapidities [17]. The similarity of enhancement in p+A and A+A collisions was also reported by HELIOS and NA35 and lack of target dependence in A+A collisions was reported by HELIOS [5, 6].

Figure 7a (top left) illustrates the contribution of various resonances to the pion spectrum in 200A GeV/c S + Pb collisions, as simulated by RQMD. The π^- arising from direct production are summed together [32]. The resonances are grouped as follows: baryonic: Δ, N^*, Δ^*; strange: K_s^o, Λ, Σ; mesonic: η, η', ω; pions from ρ's are indicated separately. Most pions at mid-rapidity arise from ρ's and primary production, while the baryonic resonances contribute more near target rapidity. Mesonic and strange resonances are of comparable importance and both peak at mid-rapidity. Figure 7b (top right) shows the pion rapidity density from RQMD for $p_T < 300$ MeV/c, corresponding to the region of the excess. Baryonic resonances clearly dominate at target rapidity, with other contributions becoming comparable at mid-rapidity. Consequently, the target rapidity peak of the low p_T enhancement is predicted by RQMD. Figure 7c (bottom left) and 7d (bottom right) show similar plots for p+Be; baryonic resonances do not play a major role in this system and hence, RQMD does not predict any strong enhancement near target rapidity.

The observed similarity between the positive and negative pion spectra indicates that the Coulomb interaction with the rest of the hadronic matter is not important in the collisions studied here. Nucleons from beam or target spectator fragments are not appearing at central rapidity. We do see a variation in the pion spectrum with centrality, though it is not strong. A weak dependence on centrality was also observed by HELIOS for negative hadrons at target rapidity ($1.0 < y < 1.9$) [5].

The lack of enhanced kaon production at low p_T further suggests that baryonic resonance decay is responsible for the excess soft pions near target rapidity. RQMD studies show that about half of the kaons arise from decays of the K* resonance, but the decay kinematics of $\mathrm{K}^* \rightarrow K$ is quite different from pions from baryonic resonances. Whereas baryonic resonances yield pions softer than the directly produced pions, there is not a large difference in p_T between the direct kaons and those from K* decay.

5 Conclusions

Ratios of p_T distributions have been used to search for enhanced π and K production at $0 < p_T < 240$ MeV/c. Within $\approx 2\sigma$, there is no difference between the π^+ and π^- spectra, and a weak dependence of soft pion production on centrality is observed. A small low p_T enhancement ($\leq 10\%$) is observed for mid-rapidity pions in p+Pb and A+A collisions, which is similar in magnitude. The enhancement in A+A collisions shows no target dependence. Excess soft pion production is smaller at mid-rapidity than at target rapidity; RQMD simulations suggest that these pions arise from baryonic resonance decay. There is no low p_T excess evident in the K^- data.

6 Acknowledgements

The NA44 Collaboration wishes to thank Heinz Sorge for access to the RQMD event generator and for fruitful discussions. We are appreciative to the staff of the CERN PS-SPS accelerator complex for their excellent work. We thank the technical staff at CERN and the collaborating institutes for their valuable contribution. We are also grateful for the support given by the Austrian Fonds zur Foerderung der wissenschaftlichen Forschung; the Science Research Council of Denmark; the Japanese Society for the Promotion of Science; the Ministry of Education, Science and Culture, Japan; the Science Research Council of Sweden; the National Science Foundation and the US Department of Energy.

References

[1] W. Bell et al., Z. Phys. C 27(1985)27
[2] T.W. Atwater et al., Phys. Lett. B 199(1987)30
[3] D. Chaney et al., Phys. Rev. D 11(1979)3210
[4] D.A. Garbutt et al., Phys. Lett. 67B(1977)355
[5] T. Akesson et al., Z. Phys. C 46(1990)361
[6] J. Harris et al., Nucl. Phys. A498(1989)133c
[7] J. Simon-Gillo, Nucl. Phys. A566(1993)175c
[8] S. Ahmad et al., Phys. Lett. B 281(1992)29
[9] T. Hemmick, Nucl. Phys. A566(1993)435c
[10] M. Gonin, Nucl. Phys. A566(1993)601c
[11] E.V. Shuryak, Phys. Rev. D 42(1990)1764
[12] M. Kataja and P. Ruuskanen, Phys. Lett. B243(1990)181
[13] S. Gavin and P. Ruuskanen, Phys. Lett. B262(1991)326
[14] L. Van Hove, CERN preprint, TH-5236/88(1988)
[15] K. Lee et al., Z. Phys. C 48(1990)525

[16] J. Sollfrank et al., Z. Phys. C 52(1991)593
[17] B. Jacak, Particle Production in Highly Excited Matter (Plenum Press, New York, 1992)471
[18] G.E. Brown, et al., Phys. Lett. B 253(1991)19
[19] E. Shuryak, Nucl. Phys. A533(1992)761
[20] W. Weise, Nucl. Phys. A553(1993)59c
[21] N. Maeda, et al., Nucl. Instrum. Methods A346(1994)132
[22] H. Beker, et al., Phys. Lett. B 302(1993)510
[23] H. Sorge, et al., Nucl. Phys. A498(1989)567c
[24] H. Sorge, et al., Phys. Lett. B271(1991)37
[25] B. Andersson et al., Nucl. Phys. B281(1987)289.
[26] B. Alper, et al., Nucl. Phys. B100(1975)237
[27] K. Guettler, et al., Phys. Lett. B64(1976)111.
[28] R. Brun et al., GEANT3, DD/EE/84-1, Data Handling Division, CERN
[29] M. Murray, et al., Nucl. Phys. A566(1994)515c
[30] J. Dodd, et al., Nucl. Phys. A590(1995)523c.
[31] D. Roehrich, Nucl. Phys. A566(1993)35c
[32] H. Sorge, et al., Phys. Lett. B289(1992)6

TABLE AND FIGURE CAPTIONS

Figure 1. Acceptance for 4 GeV/c pions and 8 GeV/c kaons in the NA44 acceptance shown in p_T versus y.

Figure 2. GEANT results showing ratio of p_T distribution of primary pions+pions from K_s^0 decays relative to primary pions.

Figure 3. Ratio of p_T distribution from central S+Pb$\rightarrow \pi^-$ as compared to S+Pb$\rightarrow \pi^+$, normalized at $240 < p_T < 320$ MeV/c.

Figure 4. Ratio of p_T distribution from central S+Pb$\rightarrow \pi^-$ as compared to peripheral S+Pb$\rightarrow \pi^-$, normalized at $240 < p_T < 320$ MeV/c.

Figure 5. Ratios of π^- p_T distributions for different projectile-target combinations, normalized at $240 < p_T < 320$ MeV/c.

Figure 6. Ratios of K^- p_T distributions for different projectile-target combinations, normalized at $240 < p_T < 320$ MeV/c.

Figure 7. a) RQMD rapidity density plot of π^- from various sources for 200A GeV/c S + Pb: $\bullet$ pions from collisions, strings and ropes; $\circ$ baryonic; $\square$ mesonic; $\star$ strange; $\triangle$ ρ's b) same plot for low p_T pions (<300 MeV/c). c) RQMD rapidity density plot of π^- from various sources for 450 GeV/c p + Be: $\bullet$ pions from collisions, strings and ropes; $\circ$ baryonic; $\square$ mesonic; $\star$ strange; $\triangle$ ρ's d) same plot for low p_T pions (<300 MeV/c).

Table 1. χ^2 per degree of freedom (χ^2/N where $N = 7$) for the ratios of p_T distributions that have been normalized to the average and fit to a line at unity.

Table 2. Observed low p_T excess for ratios of various projectile-target combinations, with and without the RQMD dN/dy corrections.

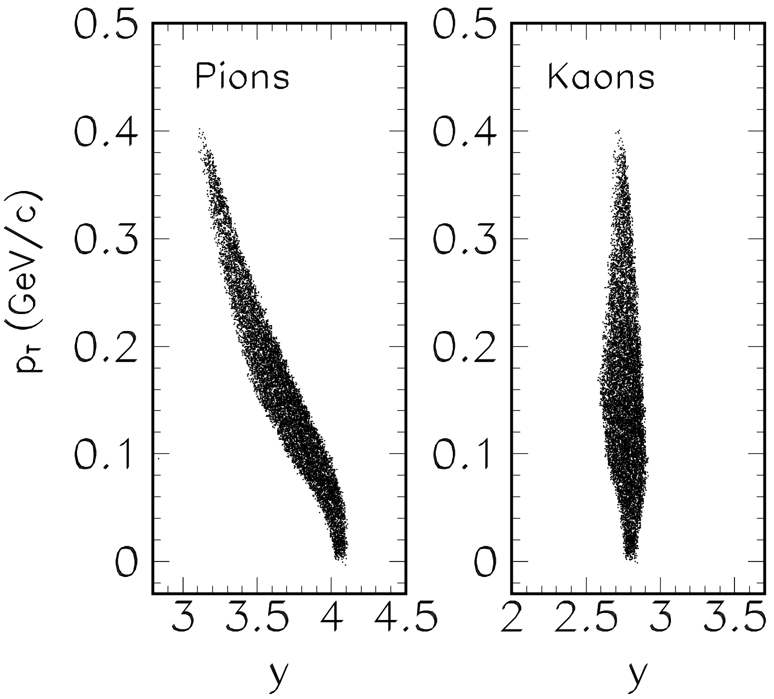

Figure 1: Acceptance for 4 GeV/c pions and 8 GeV/c kaons in the NA44 acceptance shown in p_T versus y.

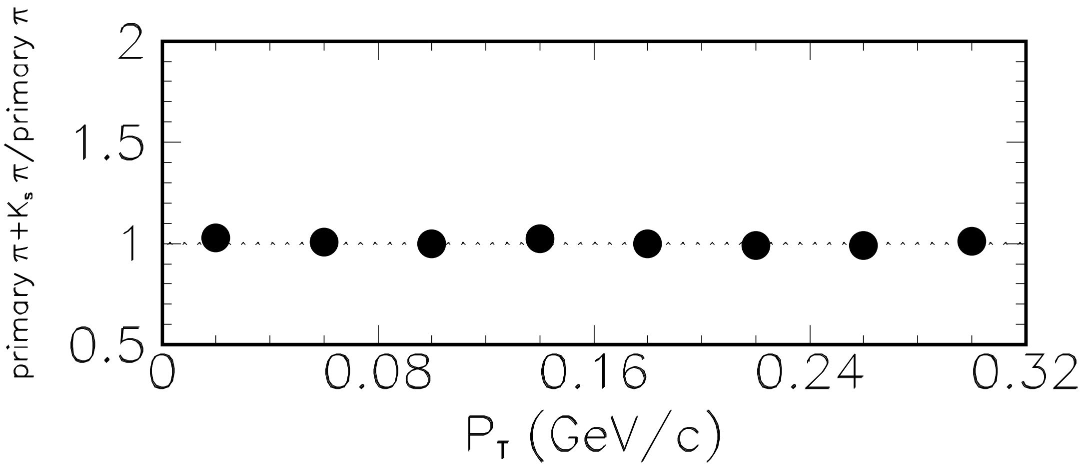

Figure 2: GEANT results showing ratio of p_T distribution of primary pions+pions from K_s^0 decays relative to primary pions.

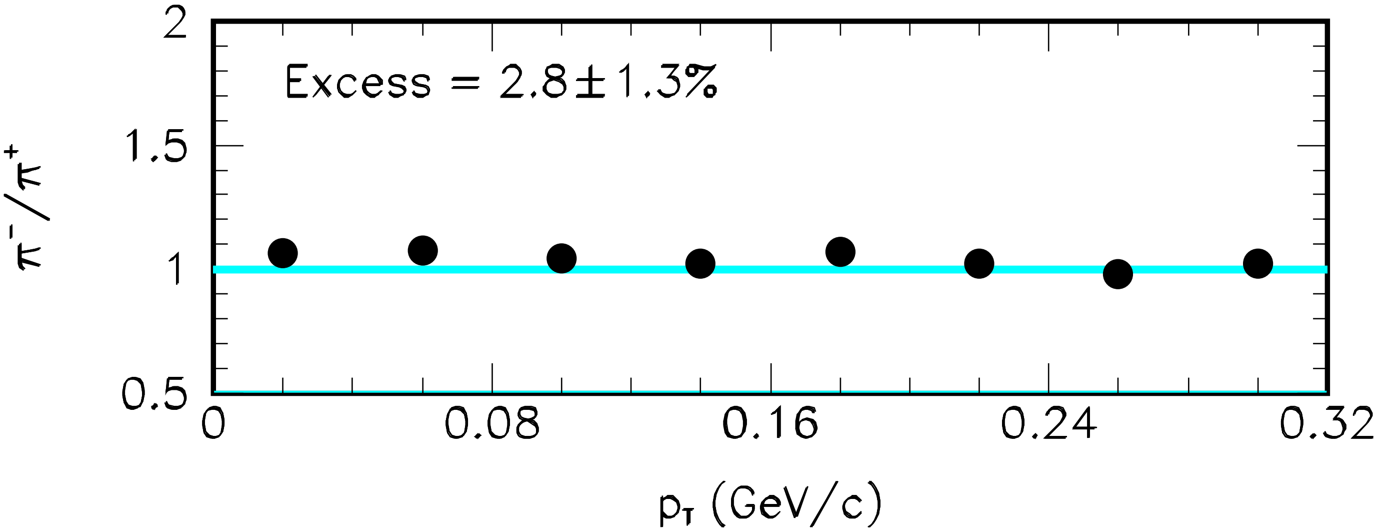

Figure 3: Ratio of p_T distribution from central S+Pb$\rightarrow \pi^-$ as compared to S+Pb$\rightarrow \pi^+$, normalized at $240 < p_T < 320$ MeV/c.

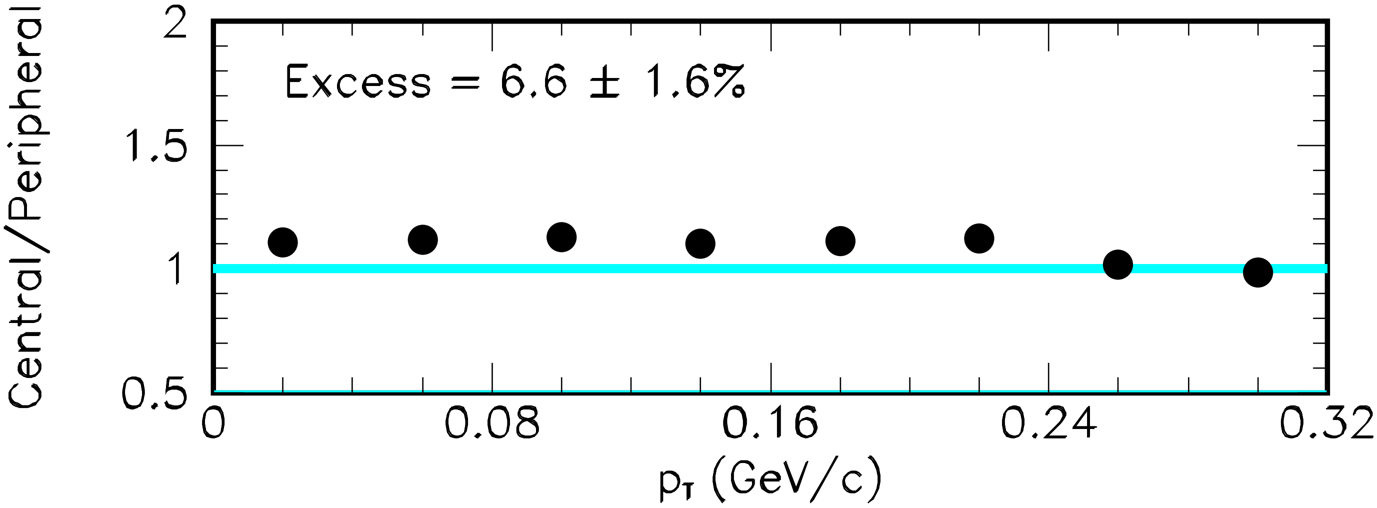

Figure 4: Ratio of p_T distribution from central S+Pb$\rightarrow$ π^- as compared to peripheral S+Pb$\rightarrow$ π^-, normalized at $240 < p_T < 320$ MeV/c.

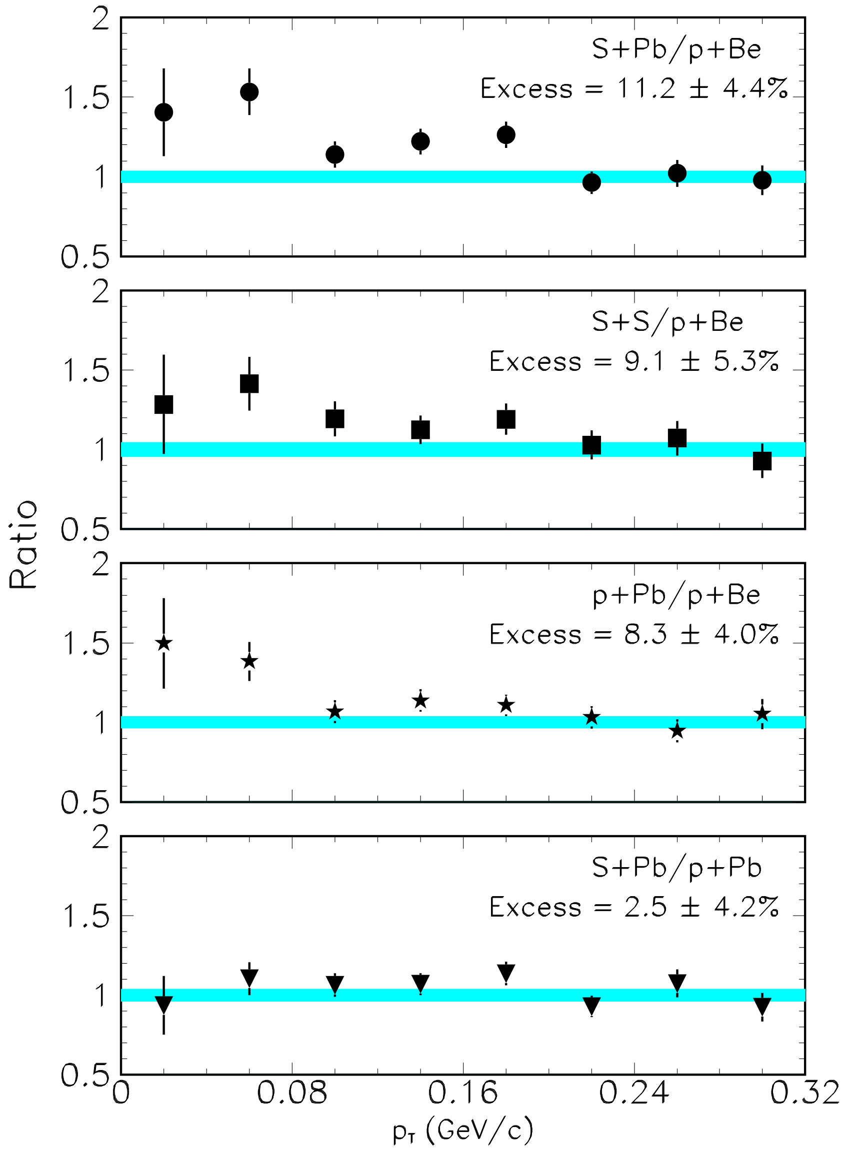

Figure 5: Ratios of π^- p_T distributions for different projectile-target combinations, normalized at $240 < p_T < 320$ MeV/c.

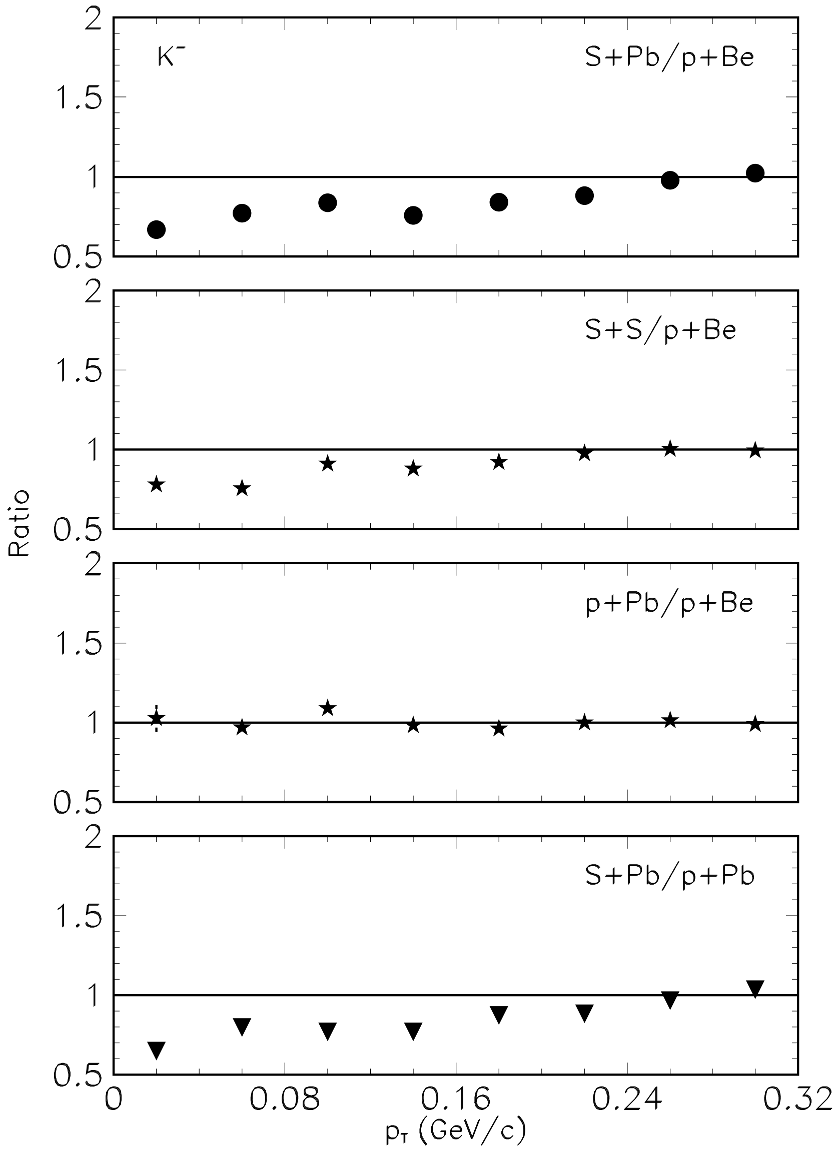

Figure 6: Ratios of K^- p_T distributions for different projectile-target combinations, normalized at $240 < p_T < 320$ MeV/c.

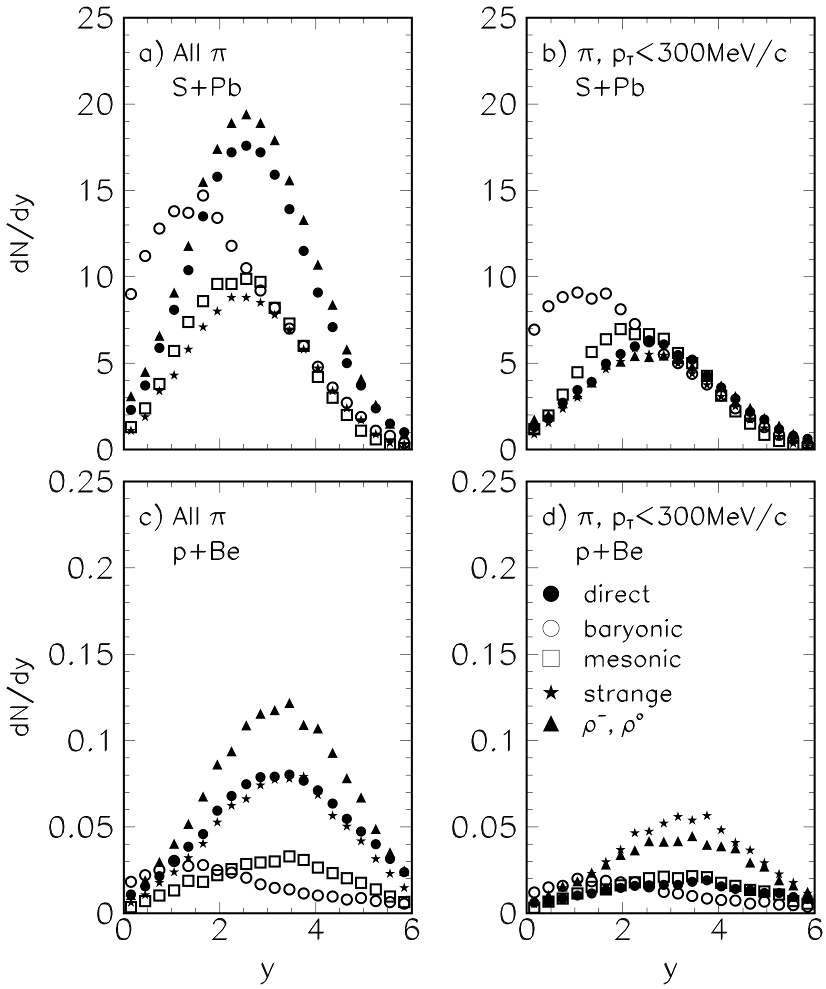

Figure 7: a) RQMD rapidity density plot of π^- from various sources for 200A GeV/c S + Pb: • pions from collisions, strings and ropes; ∘ baryonic; □ mesonic; ⋆ strange; △ ρ's b) same plot for low p_T pions (<300 MeV/c). c) RQMD rapidity density plot of π^- from various sources for 450 GeV/c p + Be: • pions from collisions, strings and ropes; ∘ baryonic; □ mesonic; ⋆ strange; △ ρ's d) same plot for low p_T pions (<300 MeV/c).